RADIO EMISSION WITH ACCELERATION OF ELECTRONS IN A POLAR GAP OF A PULSAR

V.M. Kontorovich[1,2], **A.B. Flanchik**[1]

[1]Institute of Radio Astronomy of NAS of Ukraine, Kharkov, Ukraine
[2]V.N. Karazin National University, 4 Freedom Square, Kharkov, Ukraine

Abstract. It is found that the powerful radiation, which is responsible for the radio emission of pulsars, may appear when electrons are accelerated in a polar gap by the electric field, which is assumed to be a linear function of altitude near the star surface. Averaging over the polar cap leads to a power spectrum of pulsar radio emission. We have found analytically the position of the high frequency cutoff in the radio spectra in good agreement with observations, estimated the power of radio emission and the location of low frequency turnover. We propose also an explanation for the change of the power in the main pulse and interpulse in the discussed frequency range for the Crab pulsar.

1. Introduction

Despite the efforts made during 40 years since a pulsar discovery and an appearance of huge quantity of works a mechanism of the pulsar radio emission has been still unknown. It is not clear even where there is radio emission arises – in the depth of the magnetosphere or at the periphery, near the light cylinder. Most of the proposed explanations based on the processes in the magnetosphere plasma.

We propose a new mechanism for pulsar radio emission on the basis of electron acceleration in the inner gap (Fig. 1).

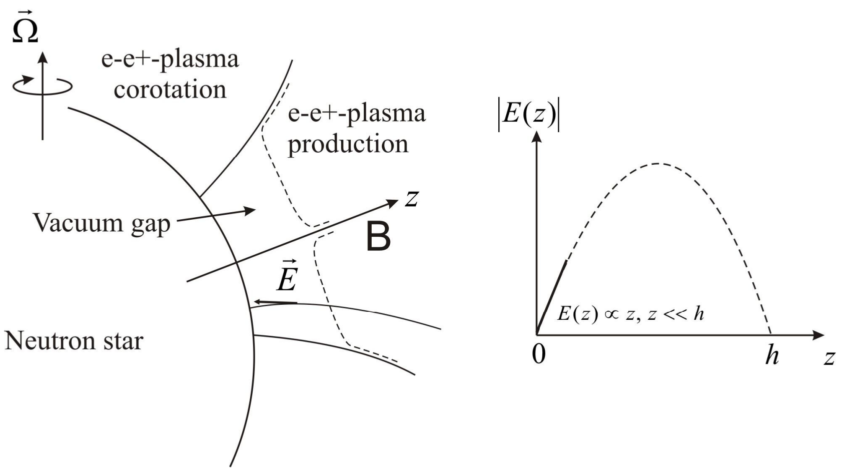

Fig.1. A polar gap scheme and accelerating field behavior.

2. Electron acceleration at initial part of trajectory in the gap

$$\frac{d\Gamma(z)}{dz} = \frac{eE(z)}{mc^2}$$ ⇦ The equation for electron Lorentz factor

$$E(z) = E_0 \frac{z}{h}, \quad \frac{E_0}{h} \sim \frac{\Omega \cdot B}{c}$$ ⇦ Accelerating electric field in the gap at low altitudes $z << h$, where h is the gap height, **E_0/h does not depend on h**

The electric field is linear on z at z << h and corresponds to free electron exit from the star surface (Scharlemann, Arons, Fawley, 1978, Muslimov, Tsygan, 1992, Harding, Muslimov, 1998). In that is our difference from Melrose, 1978, etc.

The electron acceleration in the gap is (see Fig. 2) has a sharp maximum at z_m

$$w(z) = \frac{eE(z)}{m\Gamma^3(z)} = \frac{c^2}{\Gamma^3}\frac{d\Gamma}{dz}, \quad \left.\frac{dw(z)}{dz}\right|_{z=z_m} = 0$$

$$\Gamma(z) = \Gamma_0 + a^2 z^2, \; a^2 = \frac{eE_0}{2mc^2 h}, \; \Gamma_0 \approx 1$$

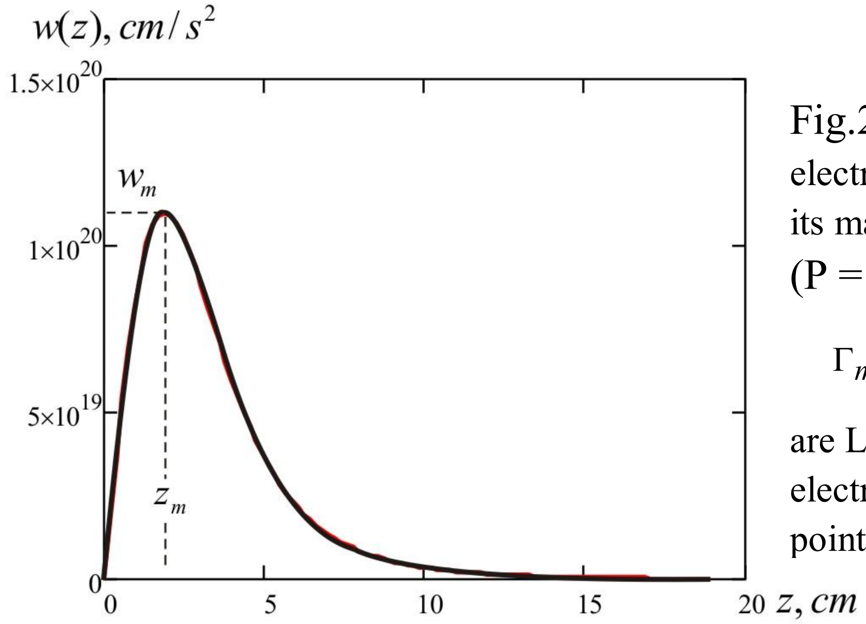

Fig.2. The dependence of the electron acceleration on z and its maximum at low altitudes (P = 1 s, B = 10^{12} G).

$$\Gamma_m = \frac{6}{5}, \quad V_m = c\frac{\sqrt{11}}{6}$$

are Lorentz factor of the electron and its velocity at the point of acceleration maximum

$$z_m = \sqrt{\frac{2mc^2 h}{5eE_0}} \approx \sqrt{\left(\frac{P}{1\,s}\right)\left(\frac{10^{12}G}{B}\right)} \cdot 1\,cm << h$$

3. Emission due to linear acceleration

The Fourier component of magnetic field of emitted wave is

$$\vec{H}_\omega = \frac{e}{c^2 R_0} e^{ikR_0} [\vec{l}, \vec{n}] L_\omega \ , \quad (\vec{l} = \vec{V} / V, \vec{n} = \vec{k} / k)$$

.

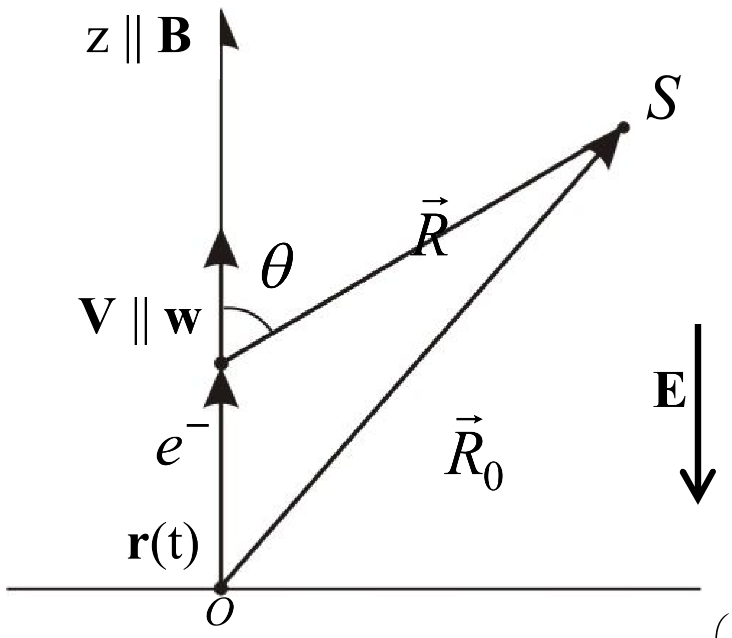

Fig.3. The emission scheme due to acceleration in the longitudinal electric field **E**.
$\cos\theta = \vec{l} \cdot \vec{n}$,
z(t) is given by the equation of motion
$\ddot{z} = eE(z)/(m\Gamma^3(z))$.

$$L_\omega = \int_0^\infty \frac{w(z(t))}{(1 - \frac{V(t)}{c}\cos\theta)^2} e^{i\omega\left(t - \frac{z(t)}{c}\cos\theta\right)} dt$$

The spectral angular distribution of the emitted energy is

$$d\varepsilon_{n\omega} = \frac{e^2}{4\pi^2 c^3} \sin^2\theta \cdot |L_\omega|^2 d\omega do.$$

From the integral L_ω it follows (numerically) that due to the fast oscillations of exponent the emitted energy falls when $\omega > \omega_{cf}$ (Fig.4). The cutoff frequency is

$$\omega_{cf} \approx \pi \sqrt{\frac{2eE_0}{mh}} = \pi \sqrt{\frac{2e\Omega B}{mc}} \ .$$

This result also can be obtained from the independent physical estimation $\omega_{cf} \approx 2\pi\, c / z_{cf}$, where z_{cf} is the altitude at which the accelerated electron becomes relativistic:

$$e \int_0^{z_{cf}} E(z) dz \approx mc^2, \ z_{cf} \approx \sqrt{\frac{2mc^2 h}{eE_0}} = \sqrt{\frac{2mc^3}{e\Omega B}}$$

(Note that $z_{cf} \sim z_m \sqrt{5}, \Gamma_{cf} = 2, v_{cf} = \sqrt{3}c/2$, where z_m is the point of acceleration maximum).

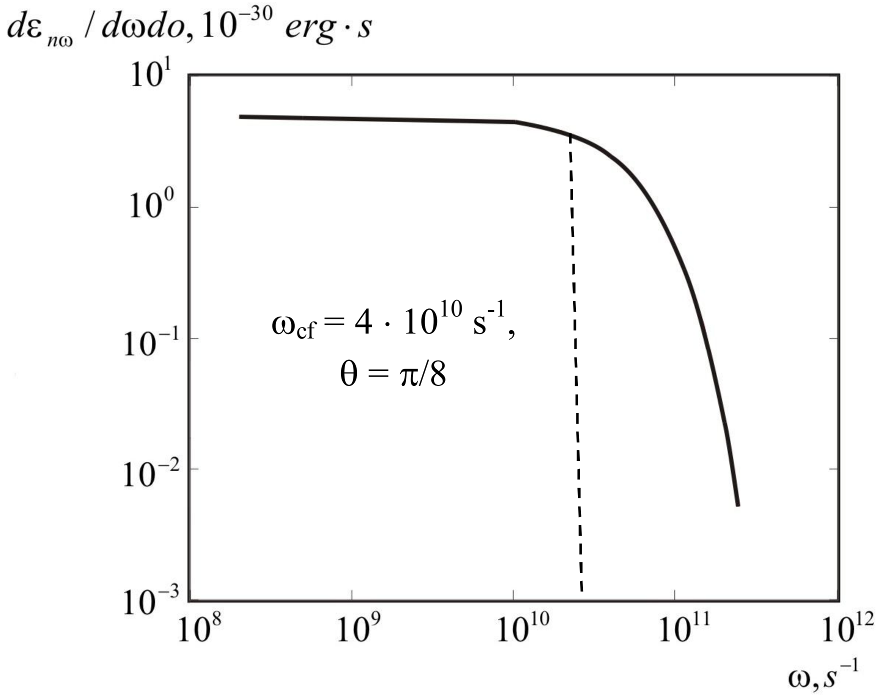

Fig. 4. The spectrum of a particle emission due to electron acceleration in the linear electric field vanishing at the star surface.

Below — a comparision theoret. and numerical estimates for $\omega_{cf}(B)$

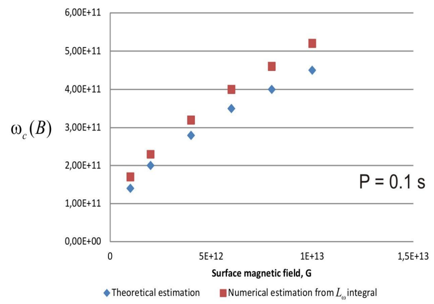

The cutoff pulsar spectra were investigated by Malofeev & Malov, 1980, who had found that the cutoff frequency for considered sample can be written as

$$\nu_{cf} \approx 1.4 \cdot 10^{9}\ Hz\ \left(\frac{1\ \ s}{P}\right)^{0.46\pm0.18}$$

(observational data Malofeev & Malov, 1980)

The our theoretical estimation of the cutoff frequency is in excellent agreement with these observational data (the average <B> for the sample is $2{\cdot}10^{12}$ G)

$$\nu_{cf} \approx 1.41 \cdot 10^{9}\ Hz \sqrt{\left(\frac{< B >}{2 \cdot 10^{12}\ G}\right) \cdot \left(\frac{1\ \ s}{P}\right)}$$

(Our prediction)

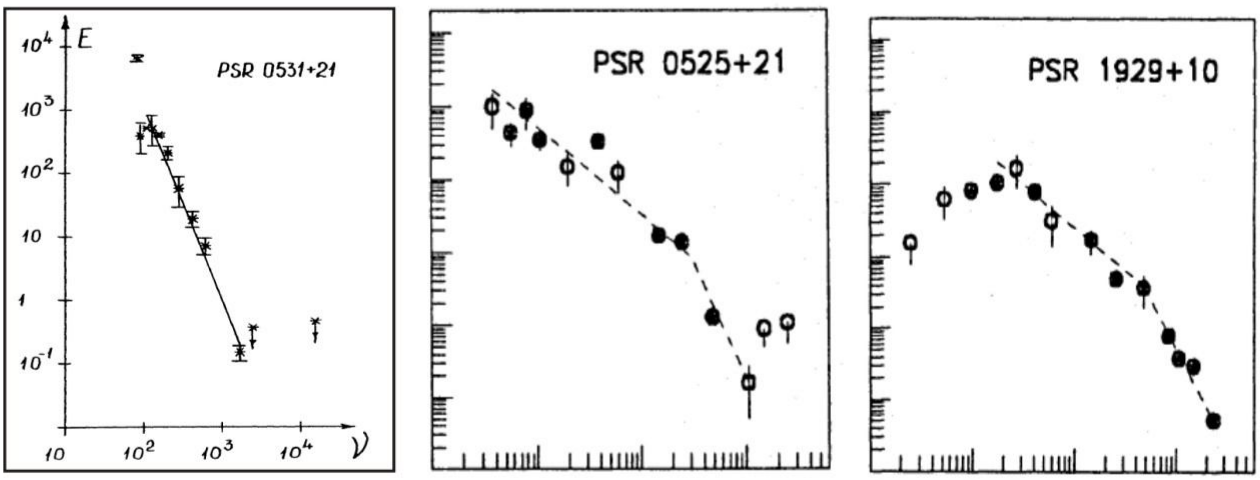

Examples of pulsar spectra (Izvekova, Kuzmin, Malofeev et al., 1981, Malofeev, Malov, 1994)

PSR 0531+21 − the pulsar in Crab −·distinguishes due to high B and short P, but small value of cosine of angle between rotation and magnetic axis (quazi-ortogonal rotator) gives the same estimates for the cut-off frequency as for pulsars from the sample.

4. Average on the surface of polar cap spectra

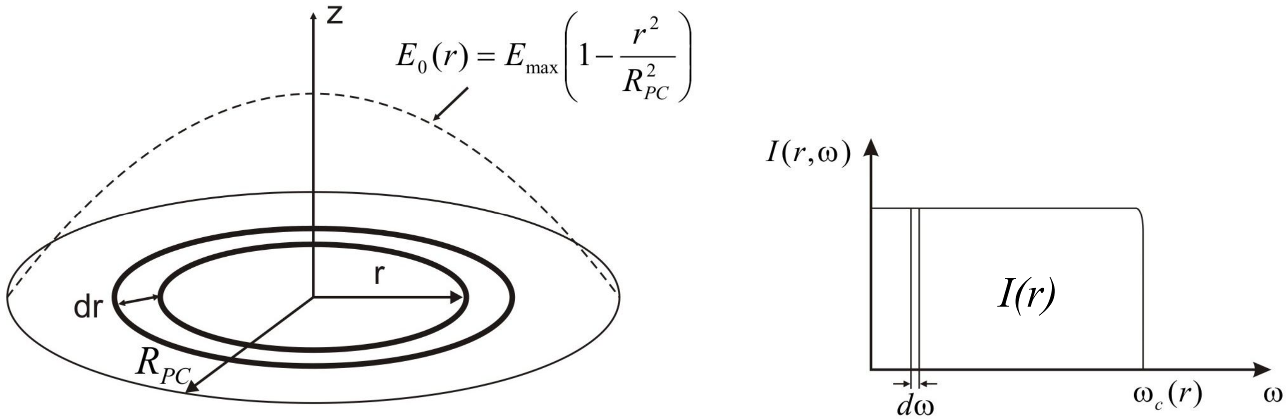

Fig. 5. The model of electric field on the polar cap (left) and using approximation of a single particle emission spectrum with cutoff on ω_{cf} (right).

The luminosity of single particle radiation is given by

$$I(r) = \frac{2e^2 w^2(r)}{3c^3} \approx \frac{e^3 E_0(r)}{mch}$$

The spectral density of energy emitted is (see Fig. 5, right)

$$I(r,\omega)d\omega = \frac{I(r)}{\omega_{cf}(r)}d\omega, \quad \omega_{cf}(r) \approx \pi\sqrt{\frac{2eE_0(r)}{mh}}$$

Taking into account the contributions from all particles at different distances from the axis z (Fig.5, left), we have for the average spectrum:

$$I(\omega) \propto \int_0^{b(\omega)} rdr\, I(r,\omega)N, \qquad b(\omega) = R_{PC}\sqrt{1-\frac{\omega^2}{\omega_{\max}^2}},$$

where N is total amount of emitting particles which is estimated from the average current through the polar cap (**incoherent case**).

The average spectrum in the **coherent case** is given by

$$I(\omega) \propto \int_0^{b(\omega)} rdr\, I(r,\omega)N_{block}(r)N_{coh}^2(r),$$

where $N_{block} \approx (R_{PC}/\lambda)^2$ is the number of coherent blocks, $N_{coh} \approx \pi\lambda^2 z_{cf}\overline{n}_e$ is the number of electrons in the coherent block, λ is the wave length. Finally

$$I(\omega) \propto \frac{1}{\omega^2}\int_0^{b(\omega)} \frac{rdr}{\sqrt{1-r^2/R_{PC}^2}} = \frac{1}{\omega^2}\left(1-\frac{\omega}{\omega_{cf}(0)}\right).$$

In this case the spectral index is near 2 – the typical spectral index of pulsars.

5. Total emission intensity estimation

The coherence provides a correct estimate of the intensity of radio emission:

$$I_R \sim N_{block} N_{coh}^2 I_1, \quad I_1 = \frac{2e^3 E_0}{3mch} = \frac{2e^3 \Omega B}{3mc^2}$$

$$N_{block} \approx \left(\frac{R_{PC}}{\lambda_m}\right)^2, \; N_{coh} \approx \pi \lambda_m^2 z_{cf} \bar{n}_e, \; \bar{n}_e \sim n_{GJ} = \frac{\Omega B}{2\pi c e}$$

$\lambda_m \sim 10^2$ cm is the wavelength corresponding to maximum in pulsar radio emission spectra, the average electron density $\bar{n}_e$ is estimated by the total current through the gap. Essencially that the only thin disk on the surface of the Polar Cap with $z<z_{cf}$ emits and for all λ inequality $\lambda > z_{cf}$ is performed. We suppose also that in the disk plane there is a fragmentation to the regions with the size less then the emitted wavelength. Finally we have the estimate for the total radio luminosity

$$I_R \sim \frac{\lambda_m^2 \Omega^3 R^3 B^2}{c^2}, \quad I_R \approx 3 \cdot 10^{27} \left(\frac{\lambda_m}{10^2 cm}\right)^2 \left(\frac{1\,s}{P}\right)^3 \left(\frac{B}{10^{12} G}\right)^2 \frac{erg}{s}.$$

which agrees well with the data on the radio luminosity of pulsars. For fast rotating Crab pulsar, which is the quazi-ortogonal rotator with large magnetic field (P = 33 ms, B = $7 \cdot 10^{12}$G) such estimate reaches 10^{31} erg/s that also agrees with observations.

6. Discussion & conclusions

1) We explain the radio emission from pulsars using a new mechanism for radiation of electrons during their acceleration by electric field in the inner gap. Significantly for that mechanism that the electric field vanishes at the surface of the star and grows linearly with altitude near the star surface.

2) Because of permanent pumping the energy density of radio emission in the gap may be quite high. That leads to gamma emission by the inverse Compton effect (Kontorovich, Flanchik, 2008) and formation of giant pulses of radiation (Kontorovich, 2010). The correlation, observed recently at the Fermi LAT between the high frequency giant pulses of PSR B0531+21 and the gamma radiation (Bilous, Kondratiev, McLaughlin, et al. 2011), also may be considered as an argument in favor of our model.

3) We have obtained the average power-law spectra of pulsar radio emission, which arise with integrating over the polar cap due to dependence of the

accelerating electric field on the electron position. The received spectral indexies are very close to the observed ones.

4) At high frequencies $\omega > \omega_{cf} \sim 10^{10} s^{-1}$ the radiation due to longitudinal acceleration falls. The received cutoff frequency agrees with observational data. At that frequency the radiation mechanisms change.

5) Changing of radiation mechanisms may explain the disappearance of the main pulse (by interpulse increasing) of PSR B0531+21 [Moffett, Hankins, 1996]. Near the cutoff frequency (Fig. 6). the radiation due to longitudinal acceleration (with wide diagram) falls with the main pulse, but interpulse rises due to contribution of the low-frequency tail of relativistic mechanisms of radiation (with a narrow radiation diagram).

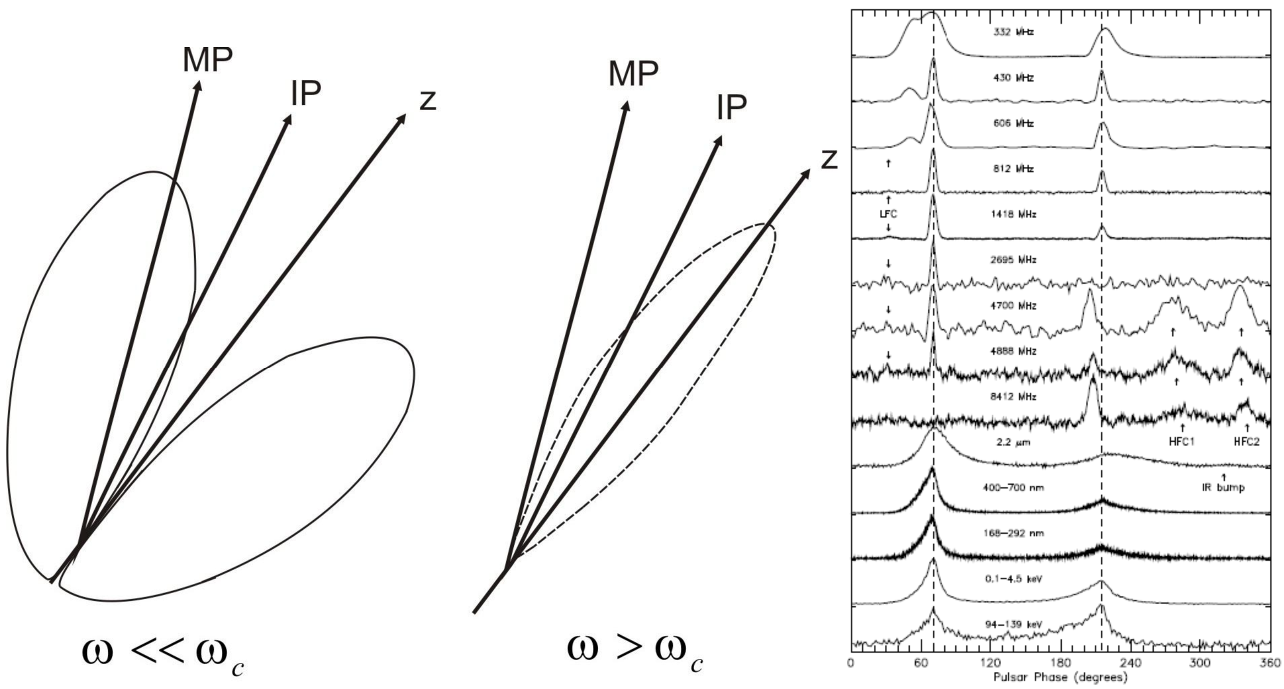

Fig.6. The scheme of the main pulse (MP) disappearance and interpulse (IP) rise for the pulsar in Crab at the cut-off frequencies due to emission changing mechanism (in projection on the 1-st quadrant, left). Multifrequency observation of Crab pulsar by Moffet & Henkins, 1996, (right).

References

V.S. Beskin. MHD Flows in Compact Astrophysical Objects, Springer, 2010.

A.V. Bilous, V.I. Kondratiev, M.A. McLaughlin et al. Astrophys.J., 728, 110, (2011), arXiv: 1101.1434 (2011).

J. Dyks, B. Rudak. A&A. 362, 1004 (2000); ArXiv: astro-ph/0006256.

A.K. Harding, A.G. Muslimov. Astrophys.J., 508, 328 (1998).

V.A. Izvekova, A.D. Kuzmin, V.M. Malofeev. Ap. Space Sci., 78, 45 (1981).

V.M. Kontorovich, A.B. Flanchik. High-frequency cut-off of spectrum and change in the mechanism of radio emission in pulsars, 28 Conference «Actual Problems of Extragalactic Astronomy–2011», http://www.prao.ru/conf/28_conf/registration/docs.php

V.M. Kontorovich, A.B. Flanchik. On the connection between the gamma and radio spectra of pulsars, Journal Exper. & Theor. Physics, 106, 869 (2008).

V.Kontorovich. Journal Exper. & Theor. Physics, 137, 1107 (2010).

V.M. Malofeev, I.F. Malov. Astron. Zhurn., 57, 90 (1980).

V.M. Malofeev, I.F. Malov. A&A. 285, 201 (1994).

I. F. Malov. Radio Pulsars. Moscow: Nauka. 2004 (In Russian).

D. Melrose. Astrophys.J. 225, 557 (1978).

D. Moffett, T. Hankins. Astrophys.J., 468, 779 (1996).

A.G. Muslimov, A.I. Tsygan. MNRAS, 255, 61 (1992).

M.A. Ruderman, P.G. Sutherland. Astrophys. J., 196, 51, (1975).

E.T. Scharlemann, J. Arons, W.M. Fawley. Astrophys.J., 222, 297 (1978).

Appendix

ACCELERATING ELECTRIC FIELD IN THE GAP

When the gap height ***h*** tends to the polar cap radius RPC ≈ R(ΩR/c)1/2 the electric field in the gap is given by (Harding & Muslimov, 1998, Dyks & Rudak, 2000)

$$E_{\|} \approx -3\frac{\Omega R}{c}\frac{B\theta_{PC}}{(1-\kappa)^{1/2}}\left(1-\frac{z}{h}\right)z\left[\kappa \;\; f_1(\xi) \;\; \cos\chi + \frac{1}{4}\theta_{PC} f_2(\xi)\sin\chi\cos\varphi\right],$$

where θPC ≈ (ΩR/c)1/2 , κ = Rg/R, χ is an angle between magnetic and rotation axes, ξ = θ/ θPC , θ is an azimuth angle measured from magnetic axis, φ is a polar angle